Simulation of Capacitively Coupled Single- and Dual-Frequency RF Discharges

Jae Koo Lee, *Senior Member, IEEE*, Natalia Yu. Babaeva, Hyun Chul Kim, Oleg V. Manuilenko, and Jong Won Shon

Invited Paper

***Abstract*—For a single-frequency capacitively coupled radio-frequency discharge, the detailed examination has been carried out of plasma density and sheath width, average potential profiles, ion-energy distribution at the electrodes and electron-energy distribution in the bulk plasma as a function of pressure, voltage, and frequency using particle-in-cell/Monte Carlo simulation. The results for Ar gas are presented. Scaling of plasma parameters with external parameters is determined. The characteristics of dual-frequency argon discharge are studied for different ratio of high/low frequencies. Nonmonotonous behavior of plasma density versus low-frequency voltages is attributed to the increase of sheath width and, as a consequence, to the increase of energy absorbed by ions in the sheath region. Subsequent decrease of energy absorbed by electrons results in the decrease of plasma density. For certain frequency ratio with the further increase of power, the plasma density increases again until the collapse of the bulk occurs.**

***Index Terms*—Capacitively-coupled plasmas, dual frequency, ion-energy distribution (IED), particle-in-cell (PIC) simulation, plasma potential.**

I. Introduction

CAPACITIVELY-COUPLED radio frequency (CCRF) discharges are receiving increasing attention due to their wide applications for thin-film deposition, etching, and plasma cleaning [1]–[3]. The extensive use of the discharges in the microelectronic industry for obtaining extraordinarily small feature sizes in etching process has motivated numerous numerical modeling of these plasma sources. In conventional CCRF, a discharge plasma is generated by driving one electrode with a single RF power source, typically at 13.56 MHz—an RF available for industrial use. Energetic ion bombardment of the substrate surface is a basic physical phenomenon that occurs in RF discharges, making them very useful as plasma-processing devices [4].

Performance of a single-frequency (SF) CCP source can be improved by finding the optimal characteristics for the discharge operation or by introducing a secondary RF source. The present paper deals with modeling in one dimension of an asymmetric discharge in a reactor operated at a conventional frequency of 13.56 MHz and higher frequencies (up to 159 MHz) at various gas pressures and applied voltages. The state of the art in modeling of asymmetric discharges for a broad range of parameters is discussed, with the specific emphases on ion-energy distribution (IED) at the powered electrode. Ion flux and ion energy play an important role for material processing as they enhance chemical etching of a surface by radicals generated in the plasma. The scaling laws which relate plasma parameters to external parameters (gas pressure, voltage, and frequency) are obtained for the case of asymmetric discharge for high applied voltages. The characteristics of dual-frequency (DF) argon discharge are investigated for a wide range of low-frequency voltages for different high-/low-frequency ratios.

The particle-in-cell (PIC)/Monte Carlo (MC) method [5] is used which is a self-consistent kinetic method capable of predicting electron energy distribution function (EEDF) with strict kinetic treatment of electrons in spatially inhomogeneous plasma and IED function for ions arriving to the electrodes. The hydrodynamic approach which treats the plasma as a fluid can give only an approximate and rough description of the phenomena in low-pressure CCRF discharges. The PIC method follows the motion of a number of superparticles. Every superparticle is composed of a large number of real particles—electrons and Ar^+ ions. The most important electron-neutral ionization, excitation, and elastic scattering processes are considered. For ion-neutral collisions resonant charge transfer and elastic scattering are taken into account.

The EEDF is an important parameter for plasma processing. Electron-impact dissociation (for molecular gases) yields radicals which are responsible for surface chemistry. The radicals produced in the bulk diffuse to the wafer, thus enhancing the surface reactions. For the considered pressure range of 20–100 mtorr, the electron–energy relaxation length is comparable to the source dimensions, and the spatial nonlocal effects are of

Manuscript received July 31, 2003; revised November 3, 2003. This work was supported in part by the LAM Research Corporation, in part by Samsung Electronics, and in part by the Korea Research Foundation under Grant KRF-2000-015-DS0010.

J. K. Lee is with the Electronics and Electrical Engineering Department, Pohang University of Science and Technology, Pohang 790-784, Korea (e-mail: jkl@postech.ac.kr).

N. Y. Babaeva is with the Electronics and Electrical Engineering Department, Pohang University of Science and Technology, Pohang 790-784, Korea, on leave from the Institute for High Temperatures, Russian Academy of Sciences, Moscow 127412, Russia (e-mail: natalie@postech.ac.kr).

H. C. Kim is with the Physics Department, Pohang University of Science and Technology, Pohang 790-784, Korea (e-mail: mindgame@postech.ac.kr).

O. V. Manuilenko is with the Electronics and Electrical Engineering Department, Pohang University of Science and Technology, Pohang 790-784, Korea, on leave from the National Science Center, Kharkov Institute of Physics and Technology, Kharkov 61108, Ukraine (e-mail: manolv@postech.ac.kr).

J. W. Shon is with the LAM Research Corporation, Fremont, CA 54538 USA (e-mail: jong.shon@lamrc.com).

Digital Object Identifier 10.1109/TPS.2004.823975

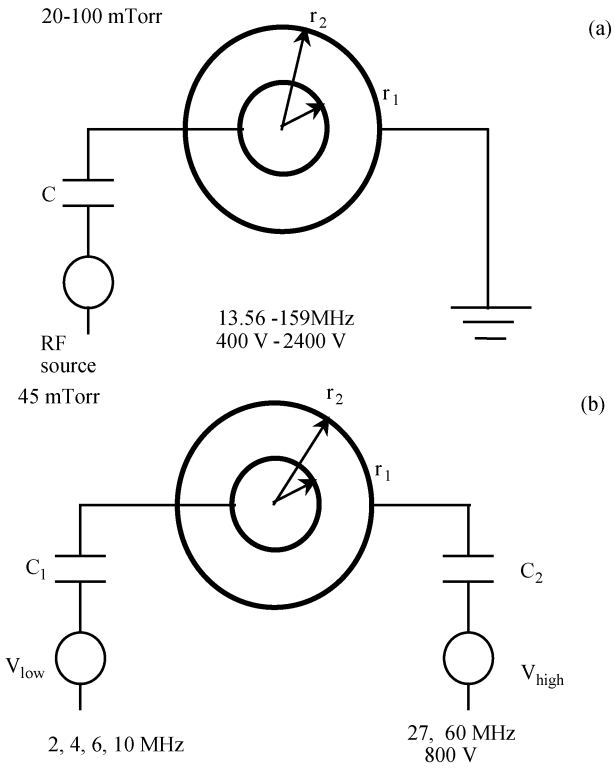

Fig. 1. Schematic diagram of the cylindrical (a) SF and (b) dual-frequency CCP sources.

great importance. Thus, EEDF is governed by the discharge properties in the whole volume. In this paper, we consider EEDF in the center of the discharge.

This paper is structured as follows. In Section II, the effect of pressure, applied voltage, and frequency on parameters of SF CCP are presented. The results and discussion on dual-frequency CCP are given in Section III, followed by the conclusion in Section IV.

II. SF Asymmetric CCP

A. Geometry for SF CCP

We have simulated the operation of an argon CCP source with cylindrical electrodes which models to the first approximation the asymmetric discharge with electrode area ratio 1.73. For this case, the inner radius of the cylindrical electrode is $r_1 = 0.0274$ m, while the outer radius is $r_2 = 0.0474$ m. The discharge is maintained in a chamber between the two electrodes separated by a gap of 2 cm, as indicated in Fig. 1(a). The inner electrode is capacitively coupled to RF power supply through a blocking capacitor. The upper electrode is grounded. Such a reactor is asymmetric in the sense that the grounded electrode is larger than the powered one. The wafer or substrate which is to be processed is placed on the inner (powered) electrode. We trace the plasma parameters along the r-axis. Distribution of ion energy is considered at the inner electrode.

B. Pressure Effect

The effect of pressure has been under investigations for decades. Surendra and Graves [6] obtained the scaling law for pressure and frequency variation for symmetric discharge. Here, we focus on asymmetric discharges. Fig. 2(a) illustrates the plasma density profiles for different values of pressure. It has been found that plasma density varies approximately linear with pressure, while the time average sheath width s (at the inner electrode) scales approximately inversely as a square root of pressure $s \propto 1/p^{0.46}$. The results are similar to that obtained in [6] for symmetric discharge. Time average plasma potential profiles for 27 MHz for two different values of pressure at a voltage of 800 V are shown in Fig. 2(b). Pressure has a minor effect on plasma potential as well as on the bias voltage at the first approximation. Plasma potential slightly increases as pressure is lowered.

Positive ions are accelerated toward the electrodes by the electric field in the sheaths. The effect of pressure on IED at the powered electrode is shown in Fig. 2(c). The IEDF is normalized on the total number of ions arriving on the unit square of the electrode. The vertical axis indicates the arbitrary units. As ions respond to the average potential, the IED spread corresponds to the mean potential drop at the electrode. With the increase of pressure the relative number of high-energy ions decreases with subsequent increase of low-energy ions. This can be attributed to the fact that with the increase of pressure the ion energy is reduced by a number of collisions. For the explanation of numerous peaks on IEDF, see [7]–[9] and references therein. Typical curves of the electron-energy probability function (EEPF) $f(\varepsilon)$ are shown in Fig. 2(d). EEPF $f(\varepsilon)$ is expressed as $f(\varepsilon) = F(\varepsilon)/\sqrt{\varepsilon}$, where $F(\varepsilon)$ is the EEDF. The electron energy ε is given in electronvolts. The amount of high-energy electrons in the bulk plasma increases as the pressure is lowered.

C. Voltage Effect

At a fixed gas pressure and RF frequency plasma density can be increased by increasing the applied voltage $V_{\rm rf}$. Fig. 3(a) illustrates the plasma-density profiles for three values of applied voltage. Plasma density increases approximately linear with voltage, the sheath width s (at the inner electrode) weakly depends on $V_{\rm rf}$ as $s \propto {V_{\rm rf}}^{0.1}$. The effect of applied voltage on plasma potential and bias voltage is presented in Fig. 3(b). There exists substantial increase in plasma potential with the increase of voltage. The self-bias voltage also increases. The applied voltage in this case is essentially dropped across the electrode sheath. This results in a wide spread of high energetic ions, as illustrated in Fig. 3(c) for $V_{\rm rf} = 2400$ V. Ion bombardment at such high energies can cause damage to the exposed surface. The EEPF shown in Fig. 3(d) is almost Maxwellian for moderate voltages. Deviation from Maxwellian distribution can be seen for high applied voltages (2400 V). The decrease in electron temperature (which can be obtained by analyzing the slopes of the curves) is observed with the increase of the applied voltage.

D. Frequency Effect

Conventional capacitively coupled discharges can achieve many advantages by operating at frequencies above the 13.56-MHz value. In the present section, the effect of frequency on discharge parameters is investigated for the broad range of frequencies from 13.56 to 159 MHz. It has been found that sheath width s scales almost inversely with frequency $s \propto 1/\omega^{0.78}$, while plasma density (center of the discharge) scales as the square of the frequency at a constant voltage and

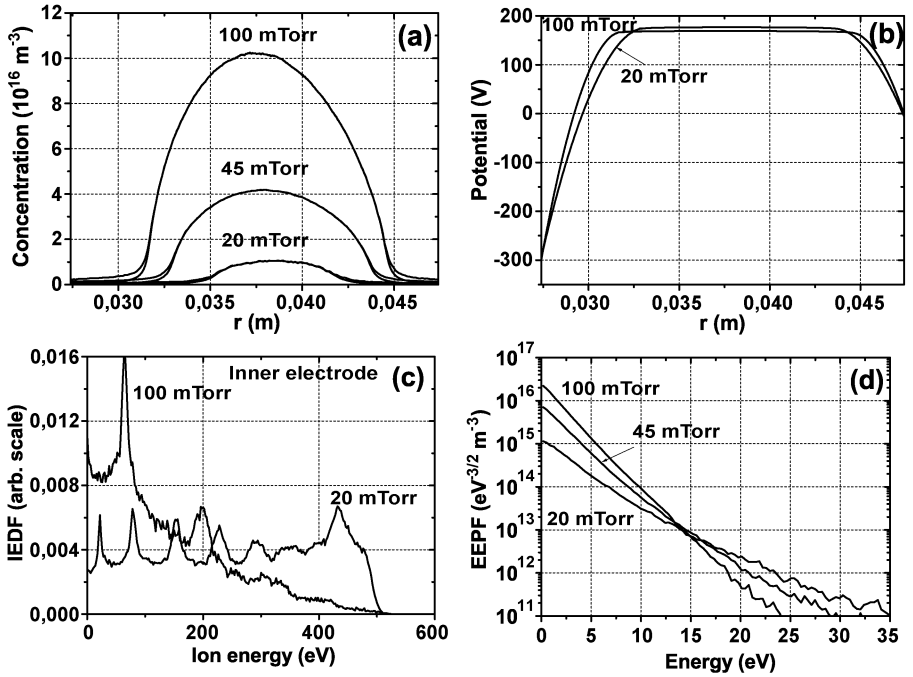

Fig. 2. Effect of pressure on (a) average plasma density; (b) average potential profiles; (c) IED at the powered (inner) electrode, and (d) EEPF. The IED spread corresponds to the mean potential drop at the inner electrode. Conditions: pressure 20, 45, and 100 mtorr, $V_{\rm rf} = 800$ V (amplitude), excitation frequency 27 MHz.

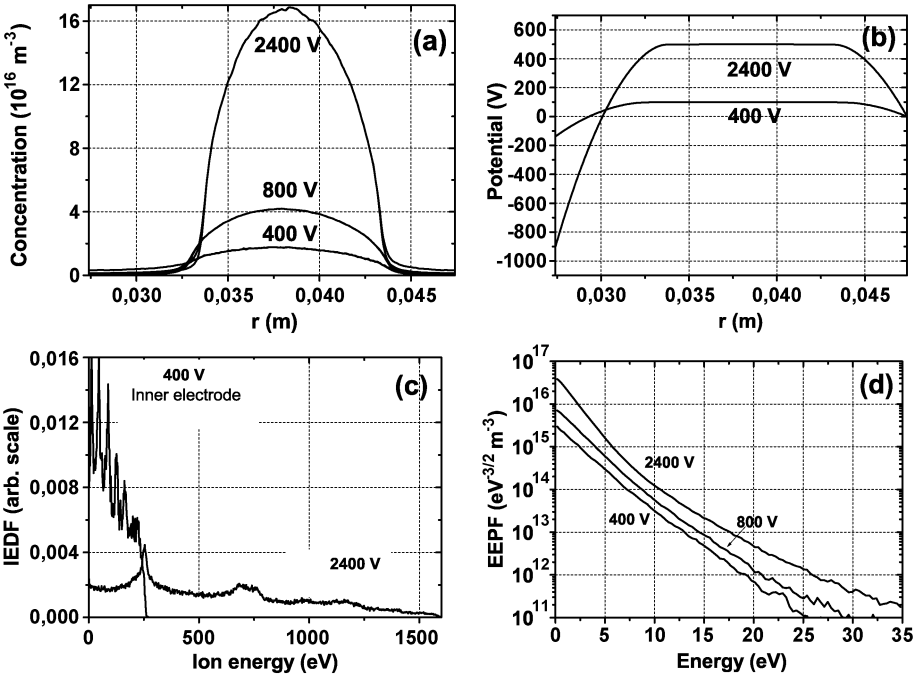

Fig. 3. Effect of applied voltage on (a) average plasma density; (b) average potential profiles; (c) IED at the inner electrode; and (d) EEPF. The IED spread corresponds to the mean potential drop at the inner electrode. Conditions: pressure 45 mtorr, $V_{\rm rf} = 400$–2400 V (amplitude), excitation frequency 27 MHz.

pressure, as illustrated in Fig. 4(a). Analogous results were obtained in [6] for a symmetric discharge (see also [10]).

The plasma potential weakly depends on frequency as shown in Fig. 4(b). With the increase of frequency, the relative number of high-energy ions arriving at the electrode increases with subsequent decrease of low-energy ions. The IED spread correlates with the mean potential drop at the inner electrode. At a very high frequency of 159 MHz, the sheath becomes rather small reducing the probability for collisions the ion experiences in the sheath. This leads to the abundance of high-energy ions, as shown in Fig. 4(c).

The EEPF presented in Fig. 4(d) is almost Maxwellian, except for the case of 13.56 MHz where EEPF can be represented as a sum of two Maxwellian distributions with two values of electron temperature. It contains extra fast and slow electrons. The relative large number of low-energy electrons in an argon discharge was observed in [11]. These excessive number of low-energy electrons is attributed to the Ramsauer

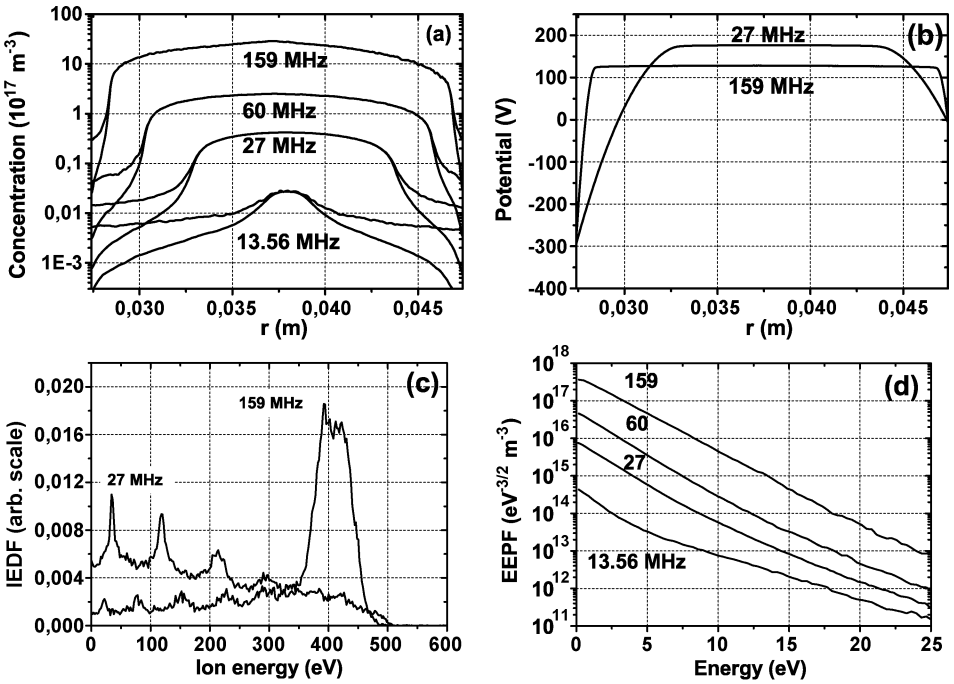

Fig. 4. Effect of frequency on (a) average plasma density; (b) average potential profile; (c) IED at the inner electrode, and (d) EEPF. The IED spread corresponds to the mean potential drop at the inner electrode. Conditions: pressure 45 mtorr, $V_{\rm rf} = 800$ V (amplitude), excitation frequencies 13.56, 27, 60, and 159 MHz.

effect which can emphasize the difference between the low- and high-energy electrons. The electron temperature weakly depends on frequency in the 27–159 MHz range.

E. Scaling Laws

Reasonably accurate scaling of plasma density and sheath width with external parameters (pressure, voltage, and frequency) can be obtained from the approximate analytical solution for power balance equation for electrons and the Child law for the dc current density for the collisional case. Following the procedure described in [1] (for the symmetric plane parallel geometry), we can write the power-balance equation for electrons as

$$P_{ohm} + 2P_{\rm stoc} = 2en_s u_s(\varepsilon_c + 2T_e). \tag{1}$$

Here, P_{ohm} and $P_{\rm stoc}$ are ohmic and stochastic heating power per unit area, n_s is the plasma density at the plasma-sheath edge, ε_c is the collisional energy loss per electron–ion pair created. For Maxwellian electrons, the mean kinetic energy lost per electron lost is $2T_e$. The factor of 2 in (1) accounts for the two sheaths. At sufficiently low pressure, ohmic heating can be neglected. The stochastic heating due to the oscillating sheaths is the main mechanism of RF power transfer at the considered pressure range [11]. For stochastic heating power, we have [1]

$$P_{\rm stoc} = C\omega^2 T_e^{\frac{1}{2}} \widetilde{V} \tag{2}$$

with $\widetilde{V} \propto V_{\rm rf}$. This expression is valid for the collisional and collisionless sheaths with different coefficients C. Simple estimations for 20–100 mtorr pressure range give $\lambda_{De} \leq \lambda_i \leq s$ (λ_{De} is the Debye length and λ_i is the ion mean-free path). In this case, we have $u_s \approx u_B \propto T_e^{1/2}$ [12]. Substituting (2) in (1), we obtain the second power-scaling law for plasma density versus frequency

$$n \propto n_s \propto \omega^2 \frac{V_{\rm rf}}{(\varepsilon_c + 2T_e)}. \tag{3}$$

For typical electron temperatures T_e of the order of 2–3 V, ε_c is much greater than T_e. Since T_e and ε_c weakly depend on pressure, they can be held constant in our consideration. For the collisional, constant λ_i sheath, the Child law for the dc ion-current density J_i can be written in the form

$$J_i = en_s u_s = \frac{C_1 V_{\rm rf}^{\frac{3}{2}} \lambda_i^{\frac{1}{2}}}{s^{\frac{5}{2}}}. \tag{4}$$

Substituting (3) into (4), we have the scaling for the sheath thickness s

$$s \propto \frac{V_{\rm rf}^{\frac{1}{5}} (\varepsilon_c + 2T_e)^{\frac{2}{5}}}{p^{\frac{1}{5}} T_e^{\frac{1}{5}} \omega^{\frac{4}{5}}}. \tag{5}$$

These results are in a reasonable agreement with PIC simulations for asymmetric discharge. For constant voltage and frequency, the analytical solution for the sheath width scales with pressure as $s \propto 1/p^{0.2}$ (PIC: $s \propto 1/p^{0.46}$). For constant pressure and frequency $s \propto {V_{\rm rf}}^{0.2}$ (PIC: $s \propto {V_{\rm rf}}^{0.1}$). For constant pressure and voltage $s \propto 1/\omega^{0.8}$(PIC: $s \propto 1/\omega^{0.78}$).

III. DF CCP

A. Geometry for DF CCP

In a conventional SF reactor, plasma density and ion energy can not be varied independently. This coupling between plasma density and ion energy is a serious limitation for conventional

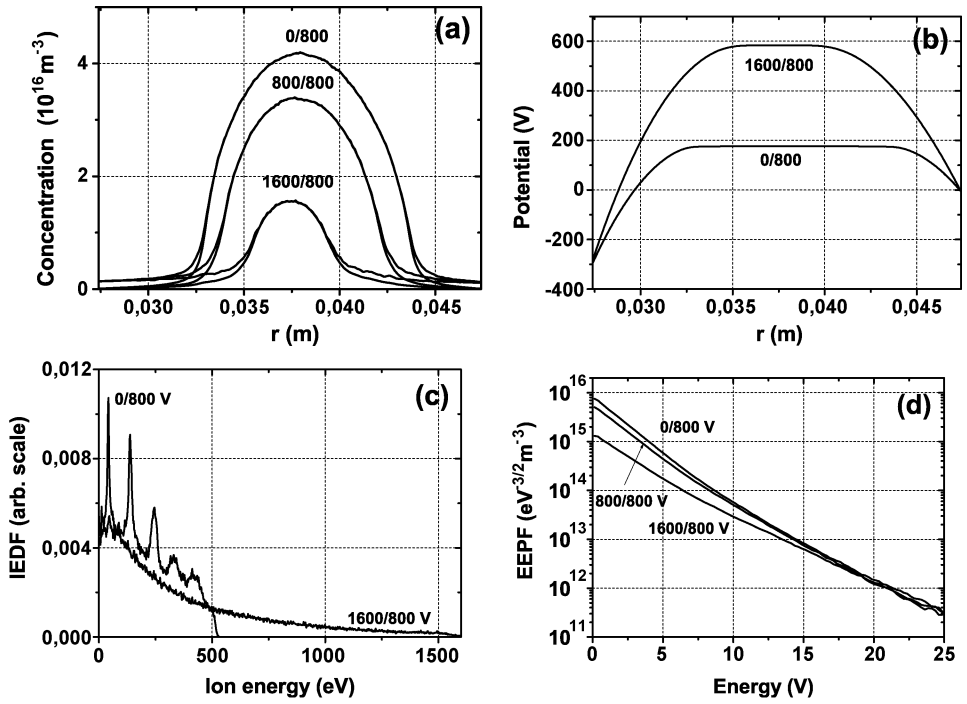

Fig. 5. Dual-frequency CCP (2/27 MHz). Effect of low-frequency voltage $V_{\rm low}$ on (a) average plasma density; (b) average potential profile; (c) IED at the inner electrode, and (d) EEPF. The IED spread does not correspond to the mean potential drop at the inner electrode. Conditions: pressure 45 mtorr, $V_{\rm high} = 800$ V, $V_{\rm low}$ is varied.

reactors. Performance of SF CCP source can be improved by introducing a secondary RF source. Such DF CCP have regained much interest in application to dielectric etch. In DF CCP, the high-frequency power source controls plasma density and, hence, ion flux to the electrode. The sheath width, plasma potential, and ion energy can be controlled by the lower frequency source [13]–[19].

The schematic diagram of the cylindrical DF CCP source is shown in Fig. 1(b). The discharge is maintained in a chamber between two electrodes separated by the gap of 2 cm. The inner electrode is capacitively coupled to power supply operating at low frequencies (2, 4, 6, and 10 MHz). The upper electrode is powered by the high-frequency source (27 MHz) at a constant voltage of 800 V (amplitude) while the lower frequency voltage is varied. In this case, the total power absorbed in the discharge increases.

B. Variation of Low-Frequency Voltage in DF CCP

For industrial purposes, it is necessary to know how plasma density, sheath width, potential drop, and corresponding IED change with the increase of low-frequency voltage. These parameters also depend on a high-/low-frequency ratio.

Fig. 5(a) shows the plasma-density profiles for frequency ratio 2/27 MHz. The increase of low-frequency voltage $V_{\rm low}$ (second power supply) leads to the decrease in plasma density with subsequent increase of sheath width until the discharge collapses. Increased plasma potential results in the increase of the IED spread, as illustrated in Fig. 5(b) and Fig. 5(c). The peaks in IED observed at $V_{\rm low} = 0$ are gradually smoothed out at $V_{\rm low} = 1600$ V. The total range of ion energies in this case does not correspond to the mean potential drop at the inner electrode as ions follow not the average but rather instantaneous

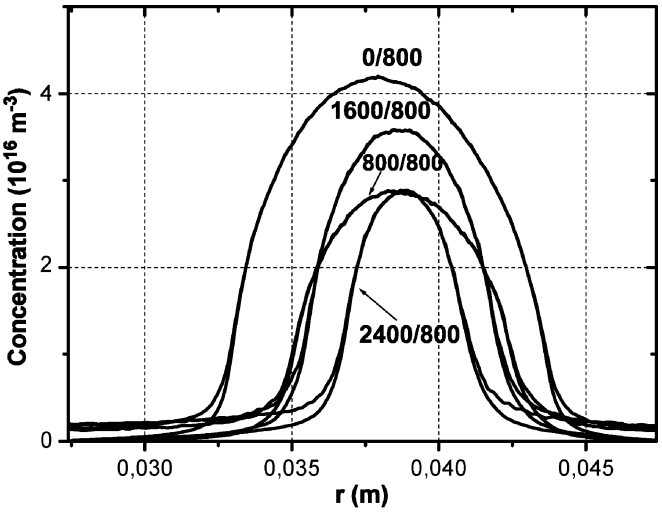

Fig. 6. Plasma density profiles for DF CCP. Conditions: 10/27 MHz; pressure 45 mtorr; $V_{\rm high} = 800$ V, $V_{\rm low}$ is varied.

potential. That results in a broader ion-energy spectrum. The previous examples show that the low-frequency controls the ion energy which is an important factor in etching process. Ion flux which governs the etch rate is independently controlled by the high frequency. Fig. 5(d) illustrates the increase in electron temperature as $V_{\rm low}$ increases.

Plasma density profiles plotted in Fig. 6 for frequency ratio 10/27 MHz demonstrate nonmonotonous behavior with the increase of $V_{\rm low}$. The profiles are shifted toward the outer electrode as $V_{\rm low}$ increases. Peak values of plasma density versus low-frequency voltage for different frequency ratio are shown in Fig. 7. The inset in Fig. 7 represents the analogous dependence for 2/60 MHz where the dip in plasma density is clearly

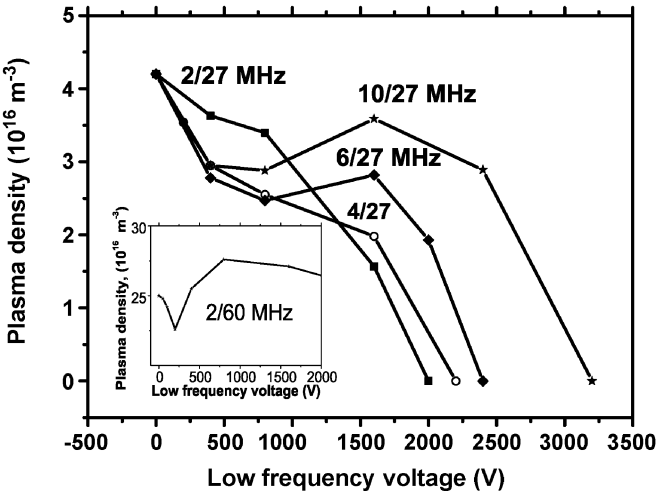

Fig. 7. Nonmonotonous behavior of plasma density versus low-frequency voltage for dual-frequency CCP. Conditions: X/27 MHz, $X = 2, 4, 6,$ and 10 MHz, pressure 45 mtorr, $V_{\rm high} = 800$ V, $V_{\rm low}$ is varied. The inset shows the similar effect for 2/60-MHz ratio.

seen. The decrease of plasma density at low voltages is related to the increase in plasma sheath width and, as a consequence, to the increase of energy absorbed by ions in the sheath region. Subsequent decrease of energy absorbed by electrons results in the decrease of plasma density. For certain frequency ratio with further increase of power absorbed by the discharge, the plasma density increases again until the collapse of the bulk occurs. More details on this subject will be given in a subsequent publication [20].

IV. Conclusion

The results discussed in this paper indicate that PIC/MC simulation provides a good physical insight into the basic characteristics of SF and DF CCP sources. The simulation model has accurate predictive capabilities on reasonable time scales.

References

[1] M. A. Lieberman and A. J. Lichtenberg, *Principles of Plasma Discharges and Material Processing*. New York: Wiley, 1994, ch. 11.
[2] F. F. Chen and J. P. Chang, *Lecture Notes on Principles of Plasma Processing*. New York: Kluwer/Plenum, 2003.
[3] T. Makabe and Z. L. Petrovic, "Development of optical computerised tomography in CCP and ICP for plasma etching," in *Advances in Low Temperature RF*, T. Makabe, Ed. New York: Elsevier, 2002, pp. 88–114.
[4] V. A. Godyak, R. B. Piejak, and B. M. Alexandrovich, "Ion flux and ion power losses at the electrode sheaths in a symmetrical RF discharge," *J. Appl. Phys.*, vol. 69, no. 6, pp. 3455–3460, Mar. 1991.
[5] C. K. Birdsall and A. B. Langdon, *Plasma Physics via Computer Simulation*. New York: Hilger, 1991, pp. 1–452.
[6] M. Surendra and D. B. Graves, "Capacitively coupled glow discharges at frequencies above 13.56 MHz," *Appl. Phys. Lett.*, vol. 59, no. 17, pp. 2091–2093, Oct. 1991.
[7] W. J. Goedheer, "Lecture notes on radio-frequency discharges, dc potentials, ion and electron energy distribution," *Plasma Sources Sci. Technol.*, vol. 9, pp. 507–516, 2000.
[8] E. Kawamura, V. Vahedi, M. A. Lieberman, and C. K. Birdsall, "Ion energy distribution in RF sheaths; review, analysis and simulation," *Plasma Sources Sci. Technol.*, vol. 8, pp. R45–R64, 1999.
[9] O. V. Manuilenko, N. Y. Babaeva, H. C. Kim, J. K. Lee, and J. W. Shon, "Ion energy distribution control in single and dual frequency capacitive plasma sources," *Plasma Sources Sci. Technol.*, submitted for publication.
[10] M. J. Colgan and M. M. Meyyappan, "Very high frequency capacitive plasma sources," in *High Density Plasma Sources*, O. Popov, Ed. Park Ridge, NJ: Noyes, 1995, pp. 149–190.
[11] V. A. Godyak and R. B. Piejak, "Abnomally low electron energy and heating-mode transition in a low-pressure argon RF discharge at 15.56 MHz," *Phys. Rev. Lett.*, vol. 65, no. 8, pp. 996–999, Aug. 1990.
[12] M. A. Lieberman, "Dynamics of collisional, capacitive RF sheath," *IEEE Trans. Plasma Sci.*, vol. 17, pp. 338–341, Apr. 1989.
[13] H. C. Kim, J. K. Lee, and J. W. Shon, "Analytic model for a dual frequency discharge," *Phys. Plasmas*, vol. 10, no. 11, pp. 4545–4551, Nov. 2003.
[14] T. Kitajima, Y. Takeo, Z. L. Petrovic, and T. Makabe, "Functional separation of biasing and sustaining voltages in two-frequency capacitively coupled plasma," *Appl. Phys. Lett.*, vol. 77, no. 4, pp. 489–491, July 2000.
[15] K. Maeshige, G. Washio, T. Yagisawa, and T. Makabe, "Functional design of a pulsed two-frequency capacitively coupled plasma in CF4/Ar for SiO2 etching," *J. Appl. Phys.*, vol. 91, no. 12, pp. 9494–9501, June 2002.
[16] S. Rauf and M. J. Kushner, "Nonlinear dynamics of radio frequency plasma processing reactors powered by multifrequency sources," *IEEE Trans. Plasma Sci.*, vol. 27, pp. 1329–1338, Oct. 1999.
[17] H. C. Kim and V. I. Manousiouthakis, "Dually driven radio frequency plasma simulation with a three moment model," *J. Vac. Sci. Technol.*, vol. A, no. 16, pp. 2162–2172, 1998.
[18] J. Robiche, P. C. Boyle, M. M. Turner, and A. R. Ellingboe, "Analytical model of a dual frequency capacitive sheath," *J. Phys. D, Appl. Phys.*, vol. 36, pp. 1810–1816, July 2003.
[19] G. Wakayama and K. Nanbu, "Study on the dual frequency capacitively coupled plasmas by the particle-in-cell/Monte Carlo method," *IEEE Trans. Plasma Sci.*, vol. 31, pp. 638–644, Aug. 2003.
[20] N. Y. Babaeva, J. K. Lee, H. C. Kim, and J. W. Shon, "Non-monotonous plasma density behavior in dual frequency asymmetric capacitively coupled plasma source" (unpublished).

Jae Koo Lee (M'83–SM'02) received the Ph.D. degree from the University of California, Berkeley, in 1979.

From 1979 to 1989, he was a Senior (later a Staff) Scientist on tokamak theory with General Atomics, San Diego, CA. He is currently a Professor in the Department of Electronic and Electrical Engineering, Pohang University of Science and Technology, Pohang, Korea. He is currently on the Editorial Board of *Plasma Source and Science and Technology*. His research interests include the theory and simulation of low-temperature basic/processing plasmas, fusion plasmas, and free-electron lasers.

Dr. Lee is the past Chair of Division of Plasma Physics of Korean Physical Society.

Natalia Yu. Babaeva was born in Klin, Moscow Region, U.S.S.R. (now Russia). She received the M.S. degree (with honors) in physics and engineering from the Moscow Institute for Physics and Technology, in 1982 and the Ph.D. degree in plasma physics and chemistry from the Institute for High Temperatures, Russian Academy of Sciences, Moscow, in 1993.

Since November 2001, she has been an Assistant Professor with Pohang University of Science of Technology, Pohang, Korea, on leave from the Institute for High Temperatures. Her research interests include physics of gas discharges, numerical modeling of low-temperature plasmas, and RF discharges.

Hyun Chul Kim was born in Gwangju, Korea, in 1976. He received the B.S. and M.S. degrees in physics from Pohang University of Science of Technology (POSTECH), Pohang, Korea, in 1999 and 2001, respectively, and is currently working toward the Ph.D. degree at POSTECH.

His current research includes the numerical modelings of plasma display panels and RF discharges.

Oleg V. Manuilenko received the Ph.D. degree in plasma physics from Kharkov National University, Kharkov, Ukraine, in 2000.

Until 2001, he was a Staff Scientist with the Theoretical Department, Institute of Plasma Electronics and New Methods of Acceleration, National Science Center, Kharkov Institute of Physics and Technology, Kharkov. He is currently a Postdoctoral Researcher with the Pohang University of Science and Technology, Pohang, Korea. His research interests include the theory and simulation of regular and chaotic dynamics of waves and particles in beam and plasma systems, X-ray sources, and plasma sources for processing techniques.

Jong Won Shon, photograph and biography not available at the time of publication.